ELSEVIER

Journal of Structural Geology 29 (2007) 209–224

JOURNAL OF STRUCTURAL GEOLOGY

www.elsevier.com/locate/jsg

The Fry method applied to an augen orthogneiss: Problems and results

Florian Genier*, Jean-Luc Epard

Institut de Géologie et de Paléontologie, University of Lausanne, Anthropole, CH-1015 Lausanne, Switzerland

Received 22 March 2006; received in revised form 22 August 2006; accepted 28 August 2006
Available online 16 October 2006

Abstract

The application of the Fry method to measure strain in deformed porphyritic granites is discussed. This method requires that the distribution of markers has to satisfy at least two conditions. It has to be homogeneous and isotropic. Statistics on point distribution with the help of a Morishita diagram can easily test homogeneity. Isotropy can be checked with a cumulative histogram of angles between points. Application of these tests to undeformed (Mte Capanne granite, Elba) and to deformed (Randa orthogneiss, Alps of Switzerland) porphyritic granite reveals that their K-feldspars phenocrysts both satisfy these conditions and can be used as strain markers with the Fry method. Other problems are also examined. One is the possible distribution of deformation on discrete shear-bands. Providing several tests are met, we conclude that the Fry method can be used to estimate strain in deformed porphyritic granites.

Keywords: Fry method; Strain; Spatial distribution; Porphyritic granite; Morishita index; Randa orthogneiss

1. Introduction

The Fry method (Fry, 1979) is a widely applied graphical technique for strain determination in rocks with rigid elements such as ooids in limestone, quartz grains in arenite, pebbles in conglomerates or phenocrysts in granite. The description of this classical and powerful technique can be found in several textbooks (for example Ramsay and Huber, 1983) and will not be explained in detail in the present paper. This method relies on a plot of the position of each particle center with respect to a particle put at the origin. The origin is then sequentially placed on each center and the relative position of every other center is plotted. This produces what is generally called a Fry diagram that shows an elliptical vacancy area around the origin (Fig. 1). This vacancy field is considered as representative of the finite strain. The powerful software package INSTRAIN (Erslev, 1988; Erslev and Ge, 1990) is currently used to perform this type of strain analysis.

This method has raised some comments on uncertainties and the validity of the resulting Fry diagram (Erslev, 1988; Erslev and Ge, 1990; Ailleres and Champenois, 1994; McNaught, 1994; McNaught, 2002; Treagus and Treagus, 2002). As pointed out by Fry (1979), the practicability and accuracy of measuring strain this way is greatly dependant of the degree and type of ordering of centers and the number of centers taken into consideration. For a homogeneously deformed set of particles and statistically isotropic and anticlustered distribution of centers, this vacancy field gives the shape and orientation of the strain ellipse (distortion). However, depending on the rock sorting and the distribution of centers, such a diagram does not always produce a clear vacancy field around its origin (Fry, 1979; Crespi, 1986; Erslev, 1988; Treagus and Treagus, 2002). Such unclear situations could lead to very approximate strain ellipse estimation and poorly reproducible results.

This paper discusses the crucial assumptions necessary to apply the Fry method. Statistical tools will be presented to give objective criteria to: (1) select a suitable population of objects, (2) choose the number of centers, (3) check the spatial distribution of centers, and (4) try to avoid artifacts and misinterpretation of the Fry diagram vacancy field. In addition,

* Corresponding author. Tel.: +41 21 692 4364; fax: +41 21 692 4305.
E-mail address: florian.genier@unil.ch (F. Genier).

0191-8141/$ - see front matter © 2006 Elsevier Ltd. All rights reserved.
doi:10.1016/j.jsg.2006.08.008

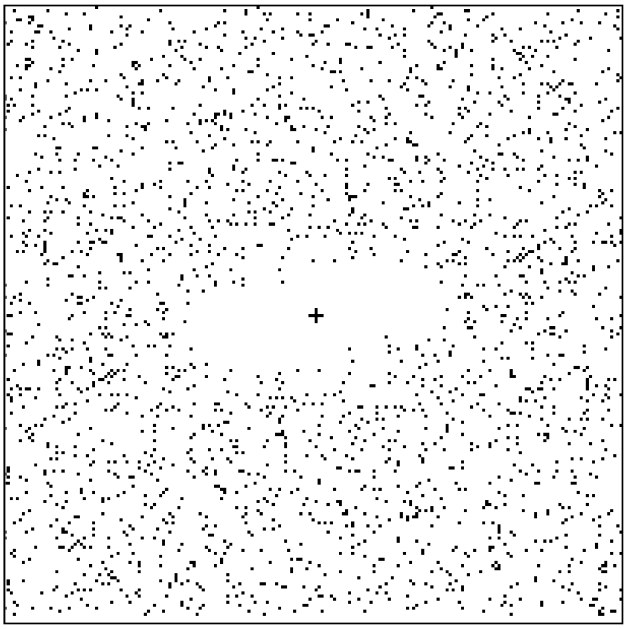

Fig. 1. A typical reliable Fry diagram. The shape of the vacancy field is regular and allows an easy estimation of the strain ellipse. The Fry diagram was obtained from 428 phenocrysts centers selected by image analysis from a picture of the Randa porphyritic orthogneiss (Western Swiss Alps).

the effect of homogeneous and heterogeneous deformation on different spatial distributions of particles will be tested. Application of the Fry method on a porphyritic orthogneiss (Randa gneiss, Siviez-Mischabel fold-nappe, Alps of western Switzerland) will be presented. We propose to systematically test the spatial distribution and to define the required minimum number of particles for the Fry analysis, in order to increase the reliability of the Fry method particularly when applied to an unpacked set of particles.

2. The Fry method and its limits

2.1. Spatial distribution of elements

In theory, the Fry method can be successfully applied only if the distribution of particles is isotropic and anticlustered. As proposed by Fry (1979) and confirmed by Crespi (1986), the more a population deviates from this type of distribution and tends to be random, the less confidence can be placed in the result. Very few publications have tested this fundamental hypothesis before using the Fry analysis. Some authors are making the assumption of such original distribution, while others use the correspondence between the result obtained from the Fry method and the inferred deformation in the studied sample to support this essential initial condition (e.g. Lacassin and Van den Driessche, 1983; Treagus and Treagus, 2002). In other words, geologically coherent results obtained with the Fry method would mean that the initial conditions with respect to object distribution are fulfilled. However, there is no objective reason why the distribution of minerals, fossils or pebbles should be always anticlustered and could not tend to be random or clustered. For example, most igneous rocks contain clusters of crystals (Jerram and Cheadle, 2000; Jerram et al., 2003). Moreover, as stated by Crespi (1986), the simple presence of a vacancy field in the center of a Fry diagram cannot be taken as a unique criterion to conclude that the spatial distribution of elements is correctly anticlustered and that the Fry method can be applied.

Knowing that the deviation from anticlustering of centers implies the decrease of the ellipse definition on the Fry diagram (Crespi, 1986; Erslev, 1988), a systematic control of the point distribution should be done for unpacked as well as for packed aggregates in order to have a better confidence in the significance of the resulting vacancy field in the Fry diagram, else difficult and even wrong interpretations can result from unclear and poorly constrained Fry diagrams.

2.2. Size distribution and sorting

Size distribution of particles is also important. Application of the Fry method to a packed and well sorted aggregate will produce an easily interpretable result. The original graphical Fry method was improved by Erslev (1988) to deal with unsorted packed aggregates. He proposed the ‘‘normalized Fry plot’’ to eliminate scatter on original Fry diagram due to variation of two-dimensional grain size. This method gives good results with packed aggregates but does not lead to any improvement with unpacked aggregates (K-feldspars in orthogneiss or pebbles in mud supported conglomerates).

In rocks with unsorted and unpacked particles, the study of size distribution will not only help to discriminate between matrix and elements, but also can provide information on what type or size of particles should preferentially be used for a Fry analysis. The division of unsorted objects in several populations of specific size range is important as each size population can display different spatial distribution. In general, spatial distribution of the largest grains tends to be the more anticlustered (Crespi, 1986). But, for relevant strain analysis, a test has to be proposed to verify that the spatial distribution of the selected centers is really satisfying.

2.3. Number of particles

The number of particles required to build a reliable Fry diagram is crucial, as a minimum number of points is necessary to define a sharp vacancy field on a Fry diagram (Fig. 1). Originally, Fry (1979) estimated this number to be a minimum of about three hundred. He used 382 centers in undeformed porphyritic andesitic lava to test the method and obtained a more or less circular vacancy field typical for an unstrained rock. Crespi (1986) described a clear dependence between the degree of anticlustering of particles and the required minimum number of them to take into consideration. According to this author, about one hundred particles would be sufficient for a very strongly anticlustered distribution, but this number increases greatly for a more random distribution. For example, in a protomylonitic granodiorite thin-section, this author calculated that a minimum of 700 K-feldspar phenocrysts would

be necessary to build a reliable Fry diagram. Substantially fewer points (227) (due to the sample size) was used and a vacancy field obtained, but with no confidence on the significance of its shape and orientation. Lacassin and Van den Driessche (1983) used 100 to 400 centers of blue quartz in an orthogneiss and obtained a good agreement between the macroscopic deformation axes and the ellipse axes deduced from the Fry diagrams. Recently, only 28 to 85 particles were used by Treagus and Treagus (2002) in tillites and conglomerates. This number seems small in comparison with the number of several hundred proposed by other authors.

In general, providing that the strain ellipses obtained with the Fry method were geologically coherent, most authors will consider that the result is reliable and no other specific tests will be performed to check the applicability of the method.

3. Spatial distribution

3.1. Definition of different types of spatial distribution

Spatial distribution of object centers in the whole rock (3-D) is out of the scope of this study, as the Fry method is basically a graphical 2-D method. In 2-D, a completely random or ''Poisson'' distribution does not imply any constraint on the position of the points. Following Poisson's law, there is no minimum distance between two points, point positions are mutually independent and the probability of finding a point at any position is constant (Kretz, 1969; Fry, 1979; Ramsay and Huber, 1983; Crespi, 1986). Such a distribution displays regions with a low density of points and others with a higher density (Fig. 2A). In contrast, clustering implies constraints on the position of points. In such a distribution, there is a greater probability that a point exists at a small distance from an existing point, than further away (Fry, 1979; Jerram et al., 1996). Such a pattern displays clearer and denser clusters than in a Poisson distribution (Fig. 2B). An anticlustered distribution implies a preferred minimum distance between points (Ramsay and Huber, 1983; Crespi, 1986), so that points are homogeneously distributed (Fig. 2C). Homogeneous (or uniform) implies that the position of a new point on a 2-D grid is dependent on its distance from already positioned points (Fry, 1979). Homogeneous distributions can be isotropic or anisotropic (Fig. 2C,D). Anisotropy means angular preferential position of points with specific spatial ordering between points.

3.2. Spatial distribution of natural objects

In rocks, due to grains size, it is impossible for the distance between two centers to be shorter than the sum of their two corresponding grain radii. In consequence, the distribution of centers in 3-D is never totally random. That is the reason why a strong anticlustering in 3-D usually results from the packing of objects with similar shape and volume. However, it is known that a random cut, even in a well-packed and sorted aggregate, could limit this anticlustering on the resulting 2-D section (Erslev, 1988). The cut plane could contain sections through the end of sphere as through the middle of sphere, so the size of the grains could vary from zero to the biggest radii of the initial spheres, with the potential effect of alteration of the strong anticlustering of centers in 2-D. Obviously, this effect increases in an unpacked and unsorted aggregate (Erslev, 1988; Jerram et al., 1996). The condition of anticlustered distribution of particles in 2-D, especially in unpacked and unsorted elements like K-feldspars in a granite, cannot be considered as fulfilled without further discussion.

For centuries many disciplines of natural sciences have been interested in methods to characterize distribution patterns. In Earth sciences, research is still focusing on spatial distribution of crystals related to magmatic and metamorphic nucleation processes (Jerram et al., 1996, 2003; Jerram and Cheadle, 2000; Mock et al., 2003). One of the first to use a variety of spatial analysis techniques to describe the distribution of crystals in a rock was Kretz (1969). Crystals were regarded to display aggregate, regular or random distributions. He found that the distribution of pyroxene, scapolite and sphene in a granulite thin-section was random. Jerram et al. (1996) used a normalization process according to the distances to the nearest neighbor centers and the modal abundance of the analyzed phase (porosity) to quantify the deviation from a random distribution of grains in the direction of a more ordered or clustered distribution. It was successfully tested on aeolian sandstones, oolitic limestones, olivines cumulates (Jerram et al., 1996); on olivines and plagioclases in lavas (Jerram et al., 2003) and on rhyolithic laccoliths (Mock et al., 2003). A cluster analysis method was also established to quantify the clustering of grains within thin sections (Jerram and Cheadle, 2000). The method, based on grain-center coordinates and grain-boundary distribution, found a clustered distribution of sphene crystals in a granulite thin section.

Despite such interest in the spatial distribution of crystals, a more general method (e.g. for unpacked aggregates, with field samples) is still missing to test isotropy and anticlustered distribution of a population of objects before using strain analysis. Consequently, we propose some simple tests that can be used prior to any strain analysis with the Fry method, to check if the type of spatial distribution of the particles is compatible with the basic assumption of the method.

3.3. Tests on spatial distributions of centers: Morishita index

The Morishita index of dispersion (MI) (Morishita, 1959) has been chosen to characterize the homogeneity of the point distributions. This index was notably used to study the clustering of earthquakes (Korvin, 1992) and in relation to environmental data (Kanevski et al., 1998; Kanevski and Maignan, 2004). To compute a MI, the entire studied area is overlaid by a regular grid, with cells of equal size. Then, the index is defined as:

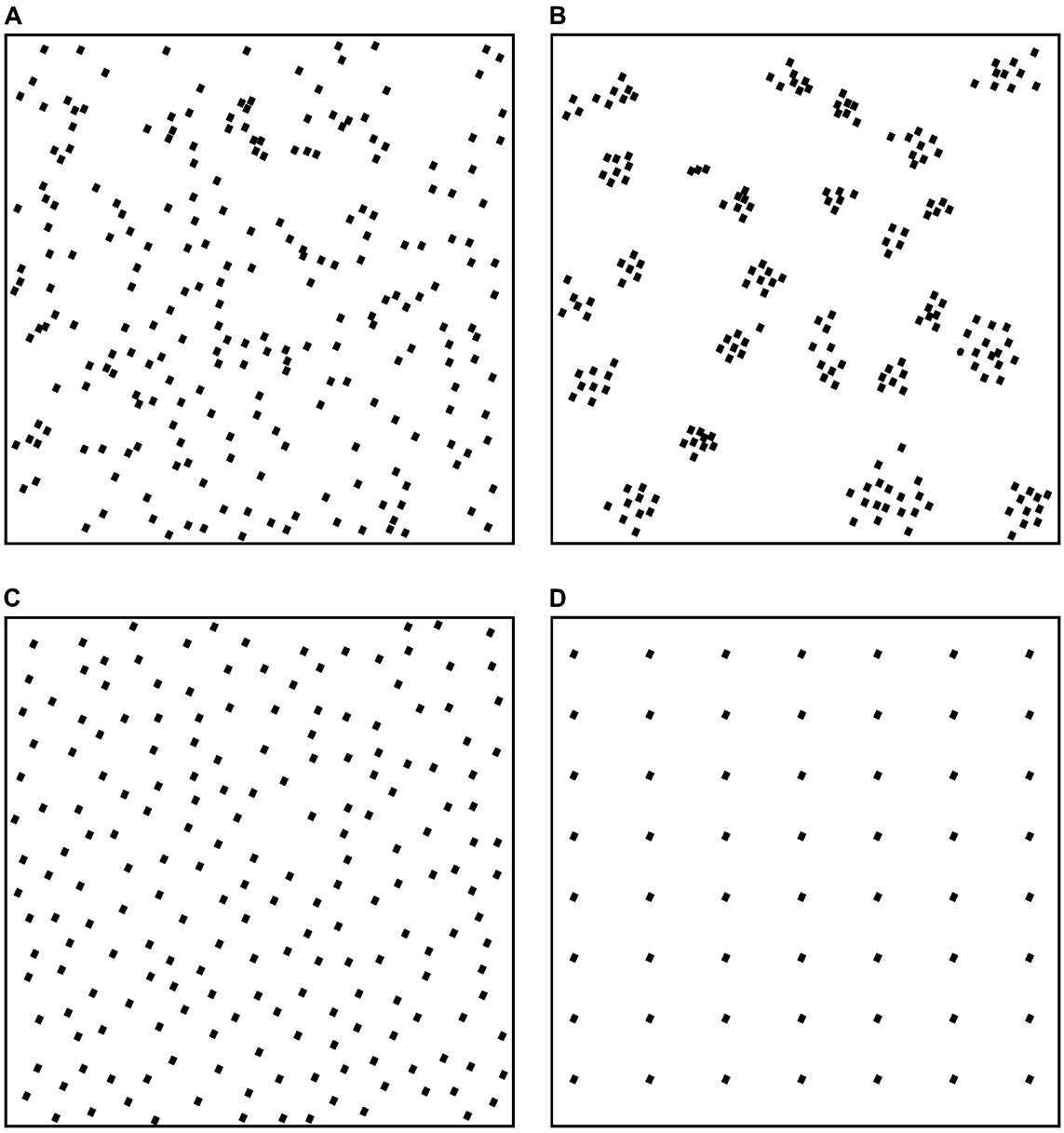

Fig. 2. Types of spatial distribution. (A) Random (Poisson), modified after Ramsay and Huber (1983); (B) clustered; (C) homogeneous and isotropic, modified after Ramsay and Huber (1983); (D) homogeneous and anisotropic.

$$\mathrm{MI} = Q\frac{\sum_{i=1}^{Q} n_i(n_i-1)}{N(N-1)}$$

where N is the total number of points, n_i ($i = 1,2\ldots, Q$) is the number of points in the ith cell and Q is the total number of cells. The type of spatial distribution, more precisely the degree of clustering, can be visualized on a graph (''Morishita diagram'') (Fig. 3) where the Morishita Index is plotted in function of the linear size of the cells (Korvin, 1992; Kanevski and Maignan, 2004). To illustrate the meaning of the Morishita index, Morishita diagrams have been built for different types of distribution (Fig. 3). For any type of distribution, if the cell size is very large and covers the entire area, the MI equal to 1 ($Q = 1$; and the totality of the particles is included in a single cell). For homogeneous distributions (isotropic or anisotropic), if the cell size decreases, each individual cell will include one element or none of them ($n_i = 1$ or 0), therefore the Morishita Index will gradually decreases from $\mathrm{MI} = 1$ for big cells to $\mathrm{MI} = 0$ for smaller cells (Fig. 3).

For a random (or Poisson) distribution, despite the cell size decrease, there will be no cell dimension for which it would be possible to put only one element in each cell. For such a distribution, the MI will vary around 1 (Fig. 3). For a clustered distribution, depending of the cell size, more than one element will be generally present in a given cell, so that $n_i \geq 2$ and the $\mathrm{MI} > 1$ (Fig. 3). For such a distribution, the MI increases with the diminution of the cell size (Fig. 3). The calculation of a Morishita diagram is the first fundamental and easy test to characterize the particle distribution prior to any Fry analysis.

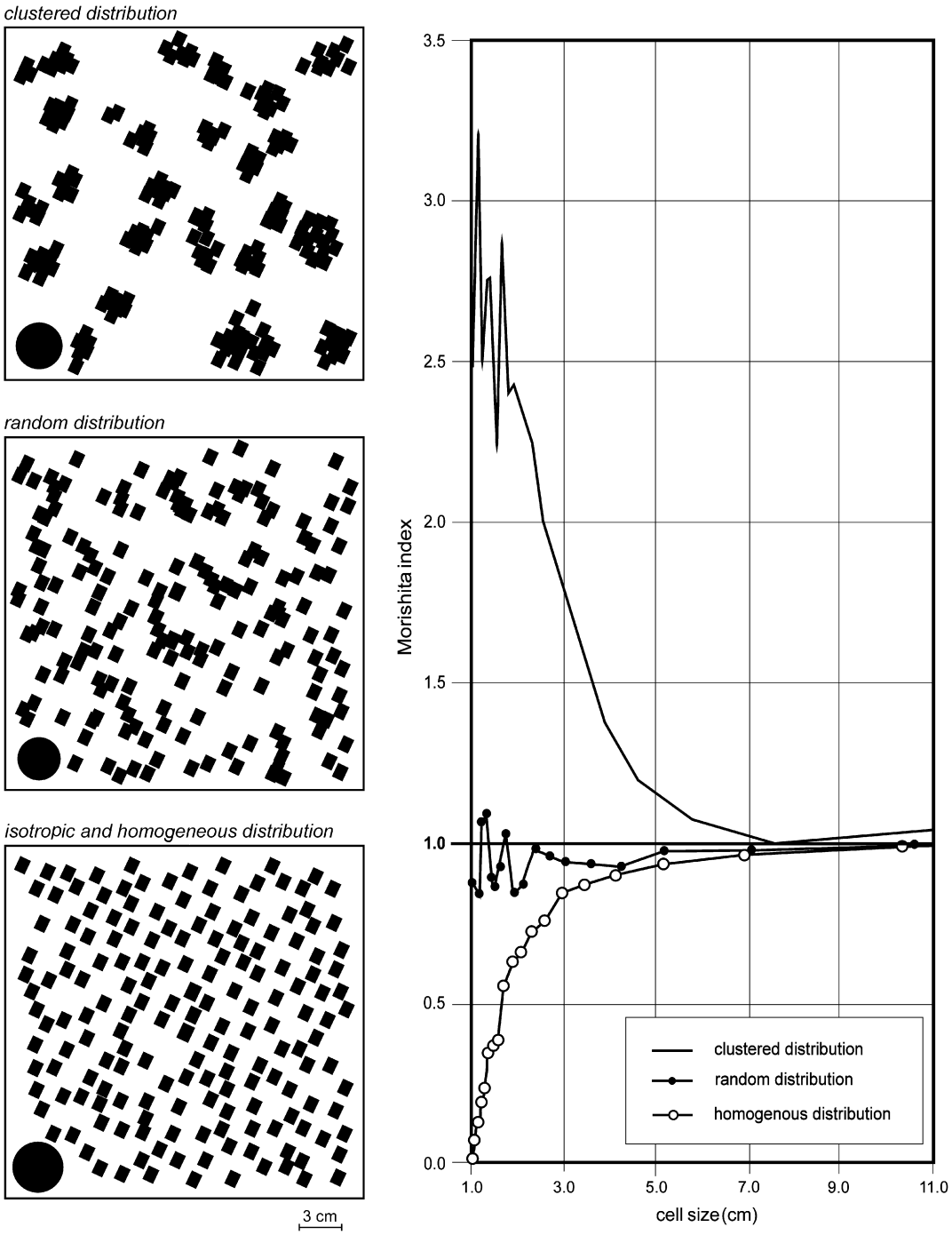

Fig. 3. Morishita diagram for a clustered, a random and an isotropic and homogeneous distribution. Morishita indexes (MI) have been calculated with the computer program "GeoStat Office" (Kanevski et al., 1998).

The Morishita test has been applied to a field view of a conglomeratic quartzite. On the resulting diagram, the Morishita index varies around 1 despite the decrease of the cell size. This result shows that the centers of pebbles are more randomly than homogeneously (anticlustered) distributed (Fig. 4). The corresponding vacancy field in the Fry diagram suggests an ellipse at high angle with respect to the foliation. As pointed out by Fry (1979), the more a population deviates from an anticlustered distribution and tends to be random, the less confidence can be placed in Fry results. Crespi (1986) also warned that using the Fry method with weakly anticlustered distribution could lead to misinterpretation of vacancy fields. Indeed, vacancy fields resulting from nearly random distribution are not always representative of the suffered strain (Fig. 5). Consequently, the ellipse obtained for the conglomeratic quartzite should be carefully interpreted in term of strain or even rejected.

In addition, as already observed in Fig. 5, the type of spatial distribution is not changed by homogeneous strains. Pure shear and simple shear were applied on clustered, random and

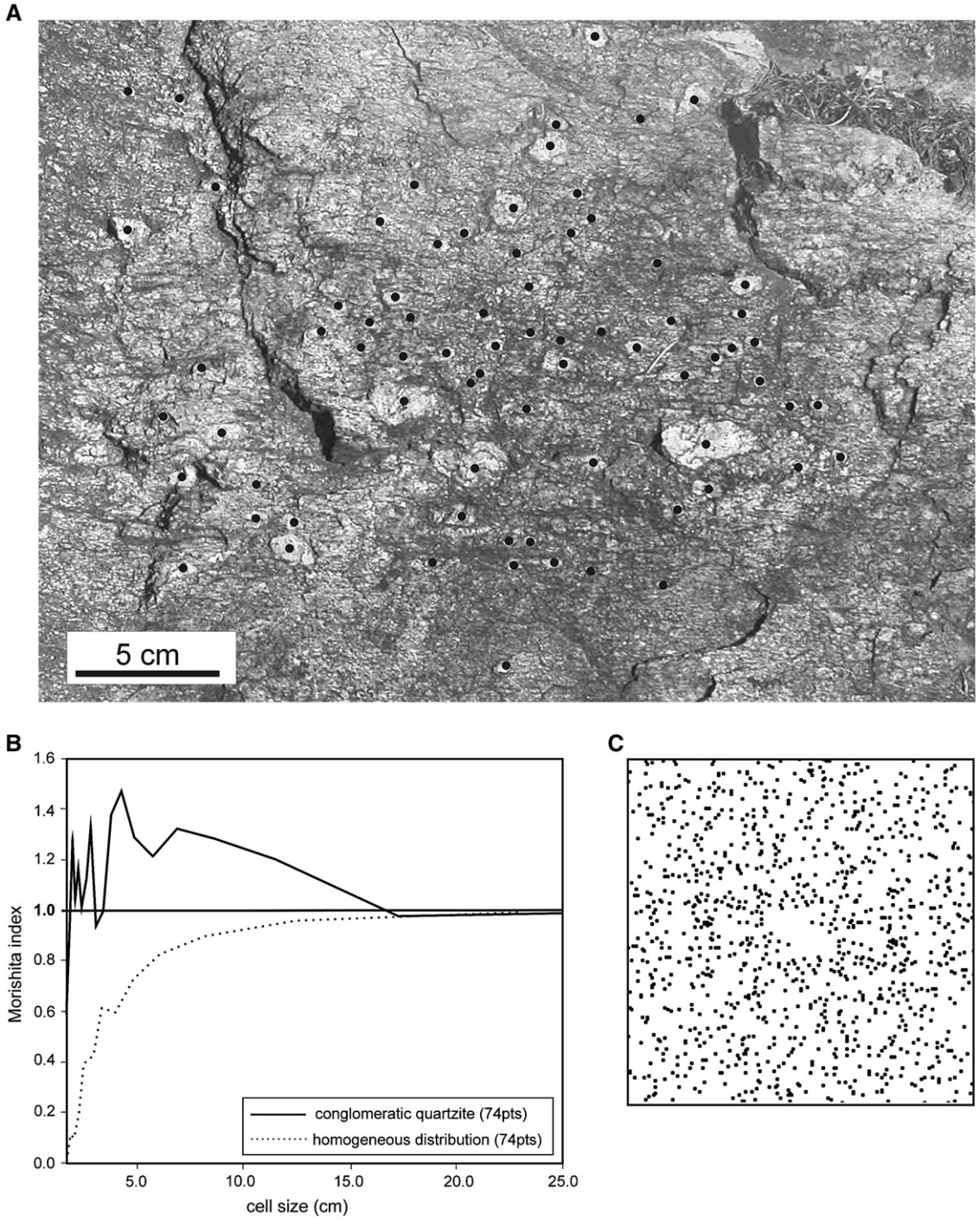

Fig. 4. (A) Outcrop picture of a conglomeratic quartzite. The black spots represent the centers of quartz pebbles used for the spatial distribution test and the Fry analysis. (B) Morishita diagram for the pebbles in the conglomeratic quartzite. The Morishita index does not decrease regularly with the decrease of the cell size, as for a homogeneous distribution. On the contrary, the index varies around 1 (random distribution). (C) Fry diagram for the pebbles in the conglomeratic quartzite. It displays a vacancy field, but, according to the spatial distribution test, the resulting ellipse should be carefully interpreted in term of strain or even rejected.

homogeneous aggregates: Resulting Morishita diagrams display similar patterns for the deformed aggregates as for corresponding undeformed ones, as presented in Fig. 6 for an isotropic and homogeneous distribution.

This test, however, does not give any information on the isotropy degree of a spatial distribution of points.

3.4. Test of isotropy

The effect of anisotropic distribution on a Fry diagram is illustrated on Fig. 7. As suggested by Fry (1979), a strained anisotropic distribution will not produce an elliptical vacancy field on a Fry diagram. For example, points regularly

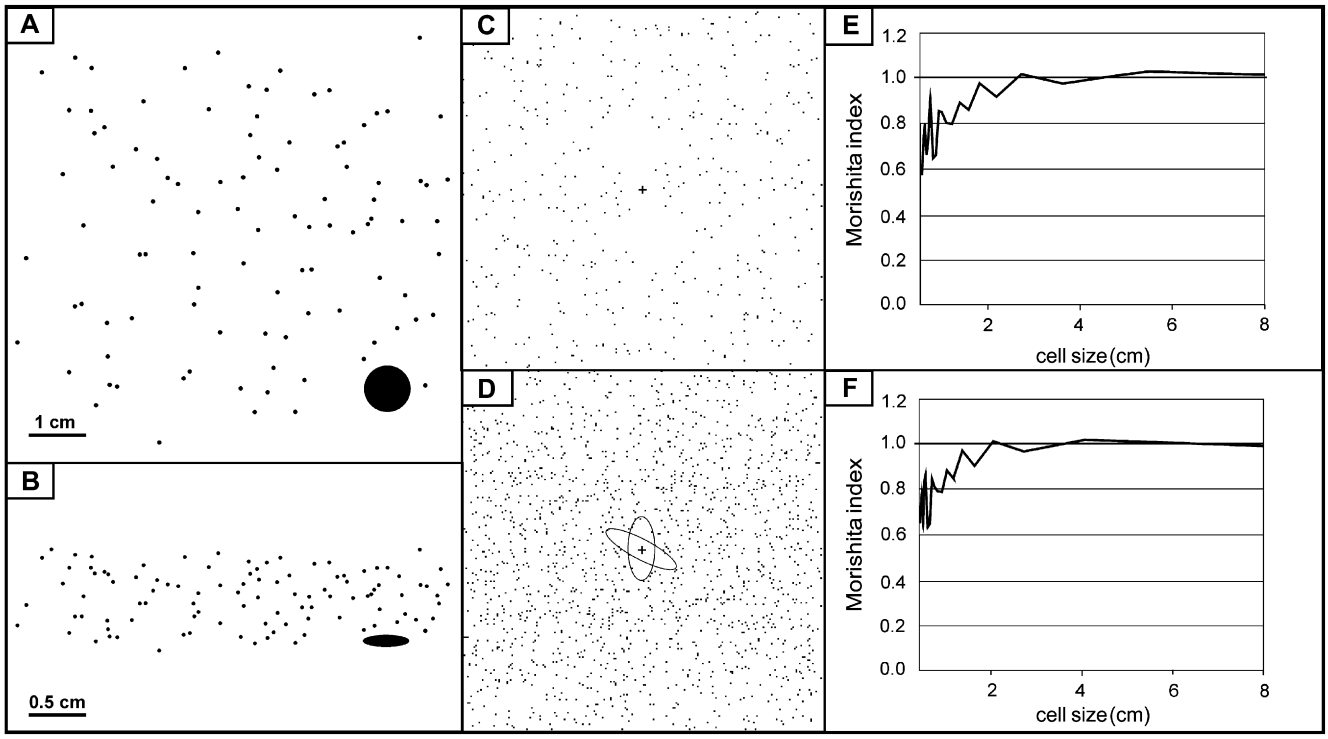

Fig. 5. (A) Generated distribution of 99 points. (B) Generated distribution (A) deformed by pure shear. (C, D) Fry diagrams for the undeformed and deformed distribution. In both cases vacancy fields are observed. The vacancy field in the Fry diagram for the deformed distribution (D) is ambiguous and can be interpreted at least in two ways, none of them in agreement with the undergone strain. (E, F) Morishita diagrams for the undeformed (A) and deformed (B) distribution. It demonstrates that the distributions differ from ideal anticlustering and tend towards random.

distributed on a square grid and deformed by a homogeneous pure shear or simple shear do not give an easily interpretable Fry diagram (Fig. 7). Sets of points have been deformed by using the software SHEAR2F (Rey, 2002). If the shear direction is parallel to the grid (horizontal or vertical) and if the γ value is equal to 1, the point distribution is totally unchanged and the Fry diagram will be totally identical to the diagram obtained from the unstrained distribution (Fig. 7A). For a γ value $= 0.5$, the vacancy field of Fry diagram could be interpreted also as circular. Pure shear (Fig. 7A′, $e_x = 1$ and $e_y = -0.5$) or other directions of the shear plane (Fig. 7B′, $\gamma = 2.74$) will lead to a similar problem and the resulting vacancy field on a Fry diagram will not give correct information on the strain ellipse.

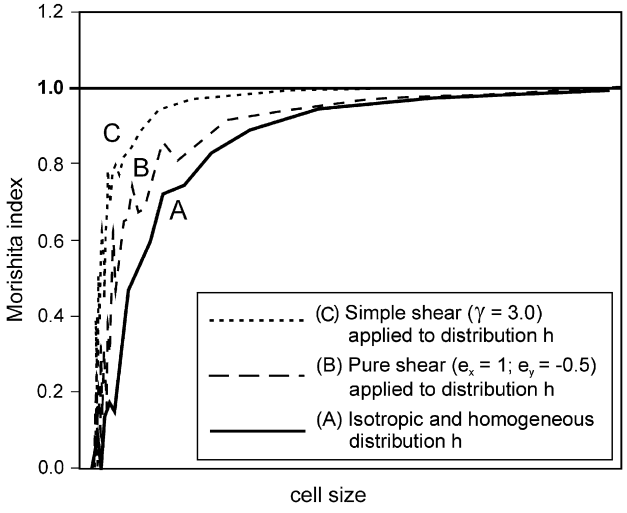

Fig. 6. Morishita diagrams for undeformed isotropic and homogeneous distribution (A), and corresponding (B) pure shear deformation ($e_x = 1$; $e_y = -0.5$), (C) simple shear deformation ($\gamma = 3.0$). The type of spatial distribution is not modified by homogeneous deformations.

In comparison, a Fry diagram for an isotropic, homogeneous and anticlustered distribution, deformed under the same condition gives good results (Fig. 8). The shape and the orientation of the ellipse deduced from the vacancy field of the Fry diagram is an excellent approximation to the strain ellipse associated with the homogeneous pure shear (Fig. 8A) and simple shear (Fig. 8B). It is also interesting to note that even for a rather high axial ratio (about 10 in Fig. 8B), the Fry method gives coherent results. In other words, if the distribution of points is clearly homogeneous, isotropic and anticlustered the Fry method is able to detect rather high strains. But, according to this test, the finite strain deduced from the Fry method, mainly for simple shear deformation, is a minimum. The deduced ellipse displays a slightly lower axial ratio ($r = 7.0$) than the true strain ellipse ($r = 9.1$). More tests should be done to evaluate this underestimation.

One simple way of measuring the degree of anisotropy is to build a cumulative histogram of the angular values between the positions of all the respective centers. For an anisotropic distribution, the angular preferential position of points will induce flats on the cumulative histogram. For example the histogram A, Fig. 9, displays significant flats on the specific 0°, 45°, and 90° angular values; on the contrary, a smooth and regular

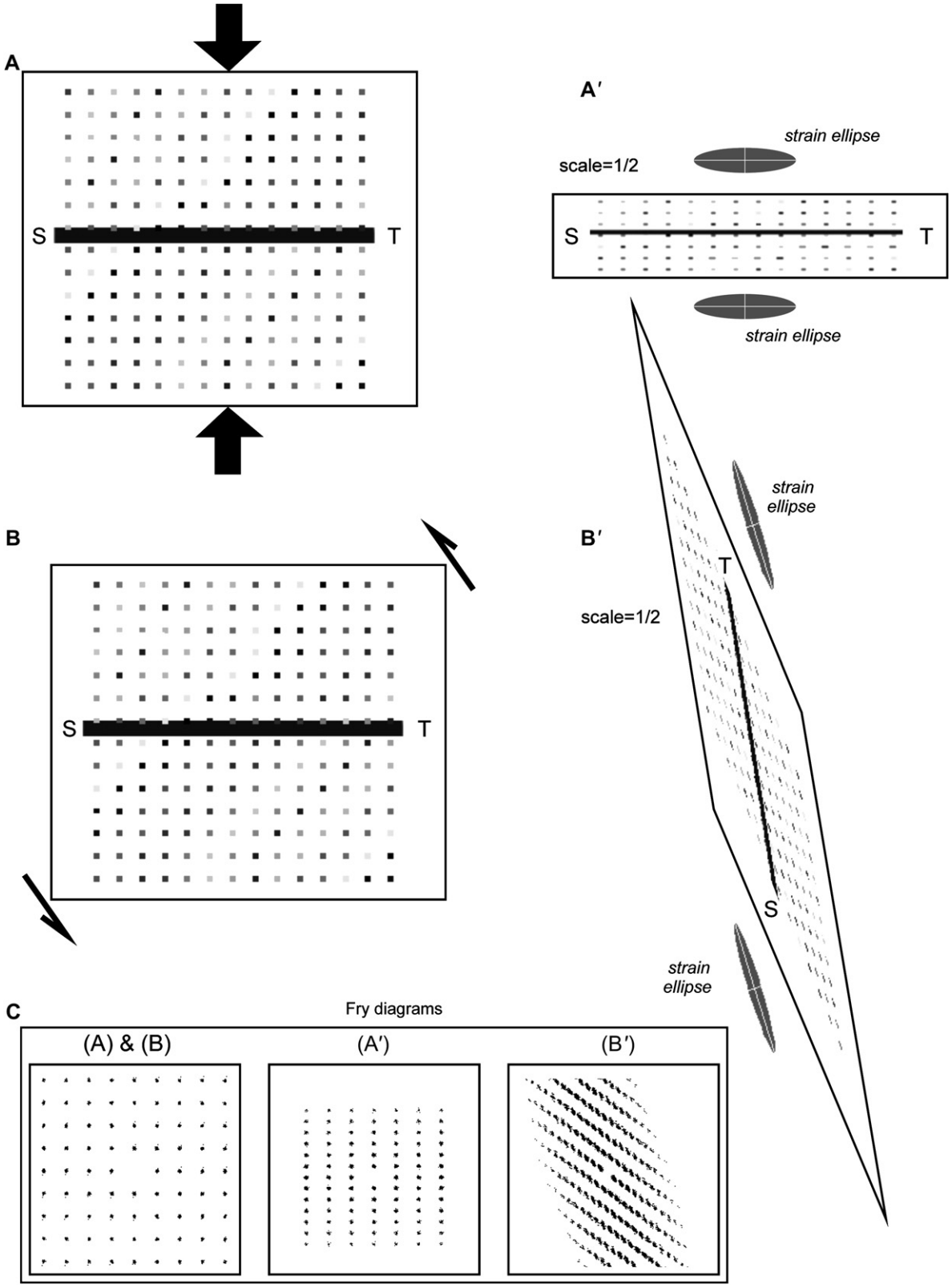

Fig. 7. Test of the Fry method on a relatively highly deformed anisotropic and homogeneous points distribution (ST: passive marker). (A, B) Undeformed situation. Deformed situation by (A′) homogeneous pure shear ($e_x = 1$; $e_y = -0.5$), (B′) homogeneous simple shear ($\gamma = \sim 2.75$). (C) Fry diagrams for: (A, B) undeformed situation, deformed by (A′) homogeneous pure shear and (B′) homogeneous simple shear. The vacancy fields are not representative of the real finite strain ellipses.

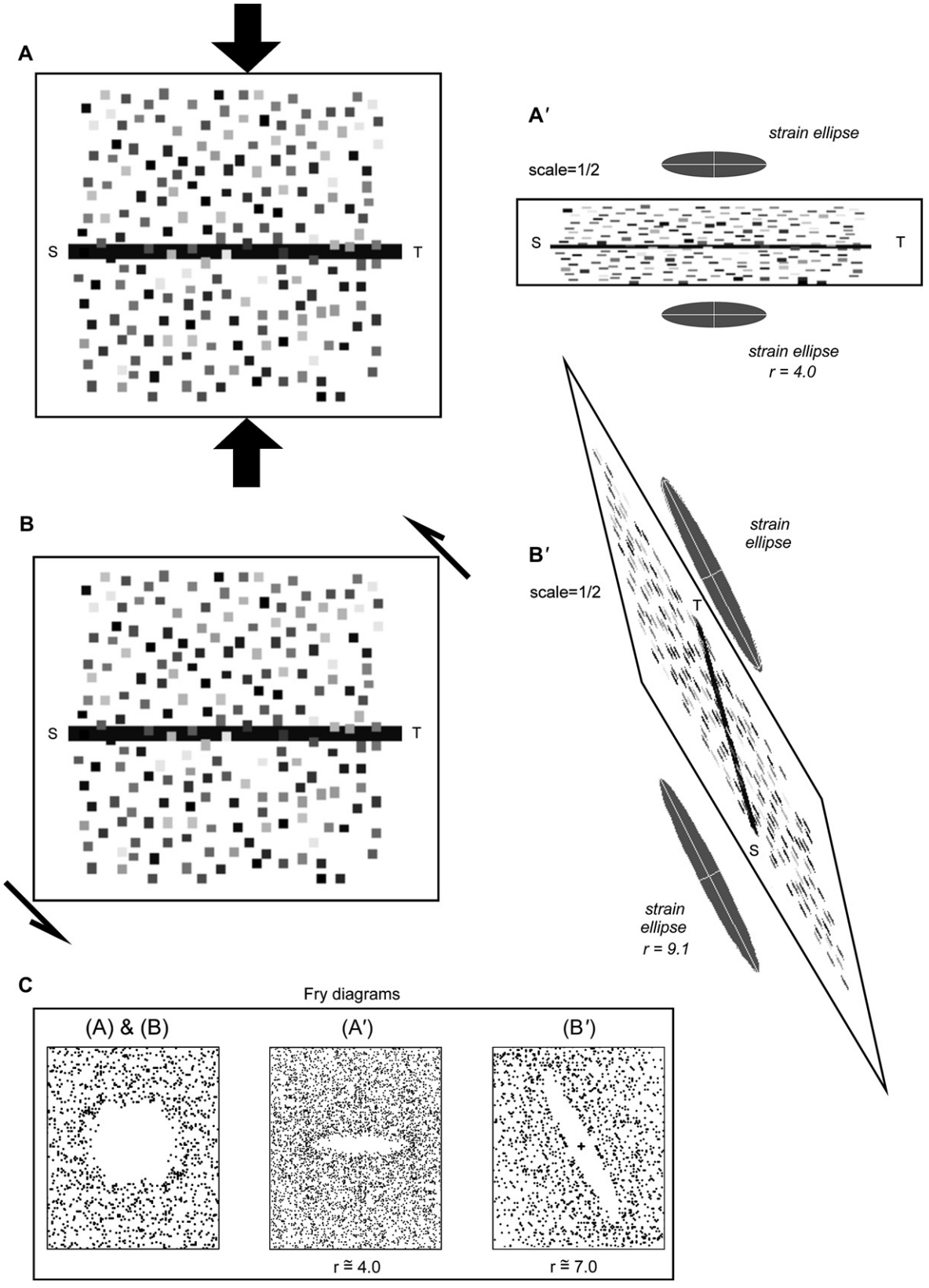

Fig. 8. Test of the Fry method on relatively intensely deformed isotropic and homogeneous point distribution (ST: passive marker). (A, B) Undeformed situation. Deformed situation by (A′) homogeneous pure shear ($e_x = 1$; $e_y = -0.5$), (B′) homogeneous simple shear ($\gamma = \sim 2.75$). (C) Fry diagrams for: (A, B) undeformed situation, deformed by (A′) homogeneous pure shear and (B′) homogeneous simple shear. The observed vacancy fields are in good agreement with the real finite strain ellipses, even if a slight underestimation occurs for simple shear.

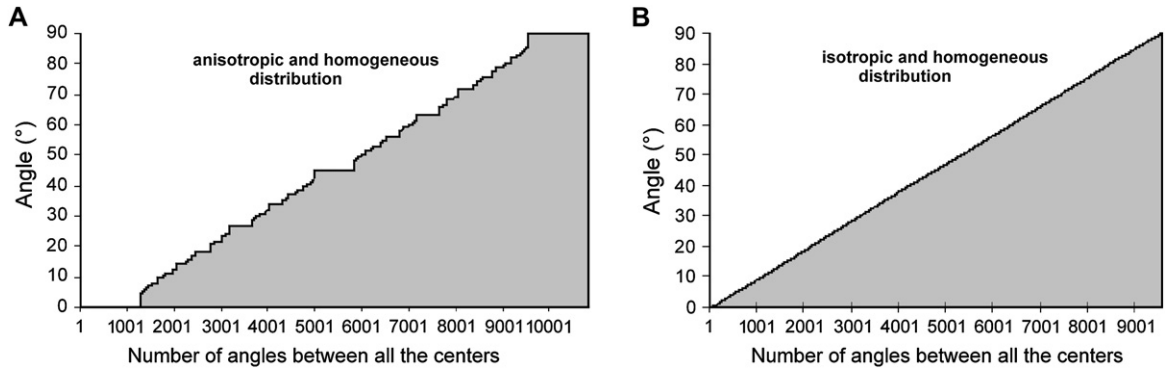

Fig. 9. (A) Cumulative histogram of the angles between each object in the anisotropic and homogeneous distribution of Fig. 2D. (B) Cumulative histogram of the angles between each object for the isotropic and homogeneous distribution of Fig. 2C.

cumulative histogram (Fig. 9B) is characteristic of an isotropic distribution (random or homogeneous).

3.5. Effects of heterogeneous deformation on a Fry diagram

Homogeneous deformation at the scale of the area considered for a Fry diagram is, by definition, a necessary condition to define a strain ellipse. In reality this condition can be difficult to check on natural examples and commonly, homogeneous deformation is simply assumed. The consequences of undetected heterogeneous deformation on strain ellipses obtained with the Fry method will be discussed.

Overgrowth of touching grains after the deformation (Jerram et al., 1996) as heterogeneous deformation of particles (Onasch, 1986; Dunne et al., 1990), particularly by pressure solution, can produce a displacement of the particle centers. In other words, centers of the deformed particles do not correspond to centers of the original particles. This will lead to an underestimation of the strain based on a Fry diagram (Dunne et al., 1990). The effects of an undetected heterogeneous deformation at the scale of the surface taken into consideration to build a Fry diagram (outcrop, sample or thin-section scale) has been poorly discussed in the literature.

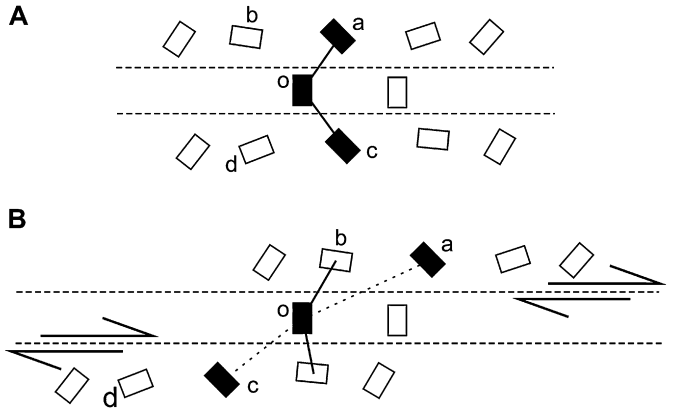

Fig. 10. Effect of heterogeneous shearing along discrete shear planes (dashed lines). (A) Initial situation. (B) Deformed situation. Mean distance between markers (i.e. K-feldspar phenocrysts) located between two successive shear planes will not be changed. In addition, the nearest feldspar (a) from a given feldspar (o) in the initial distribution would migrate away, so that another feldspar (b) would become the nearest neighbor of the given feldspar (o). The strain induced by this type of structure will be therefore greatly underestimated or even ignored by the Fry method.

A first effect of heterogeneous deformation is illustrated on Fig. 10. A set of objects (for example K-feldspar phenocrysts) is deformed by discrete shear-planes. This type of heterogeneous deformation will slide undeformed ‘‘trains’’ of objects along the shear planes in such a way that, for large a deformation, it will be impossible to detect the initially neighboring objects. In other words, for increasing deformation, in Fig. 10B, the objects a and b can be translated out of the picture. The overall distribution of objects will not be drastically modified and therefore the deformation will be largely underestimated, or even will remain undetected. Rather, small displacements on the shear planes will result in a Fry diagram difficult to interpret as illustrated in Fig. 11.

Fig. 11A shows the original homogeneous and isotropic distribution of objects. The resulting Fry diagram displays a clear circular vacancy field. A displacement equivalent to half of the mean distance between individual objects was applied to discrete shear planes, first with a constant shear sense from base to top (Fig. 11B) and secondly with periodic reversal of the shear sense (Fig. 11C). An ellipse with small eccentricity can be fitted into the vacancy field of the two resulting Fry diagrams. These ellipses are, however, not significant with respect to the deformation. In a natural sample, for example in an augengneiss, the interpretation of the rock foliation has to be discussed before applying the Fry method.

In summary, before the application of the Fry method to an unpacked aggregate, two types of questions have to be addressed. The first type is related to particle distribution (isotropic and homogeneous). The tests presented in this paper should bring the necessary answer. In the following section they will be applied to the Randa porphyritic orthogneiss. The second type is in a way more crucial as it is related to the basic assumption of homogeneous deformation to define a strain ellipse. No clear and unambiguous answer can be determined here, but this basic hypothesis has to be kept in mind when interpreting the result of a Fry diagram.

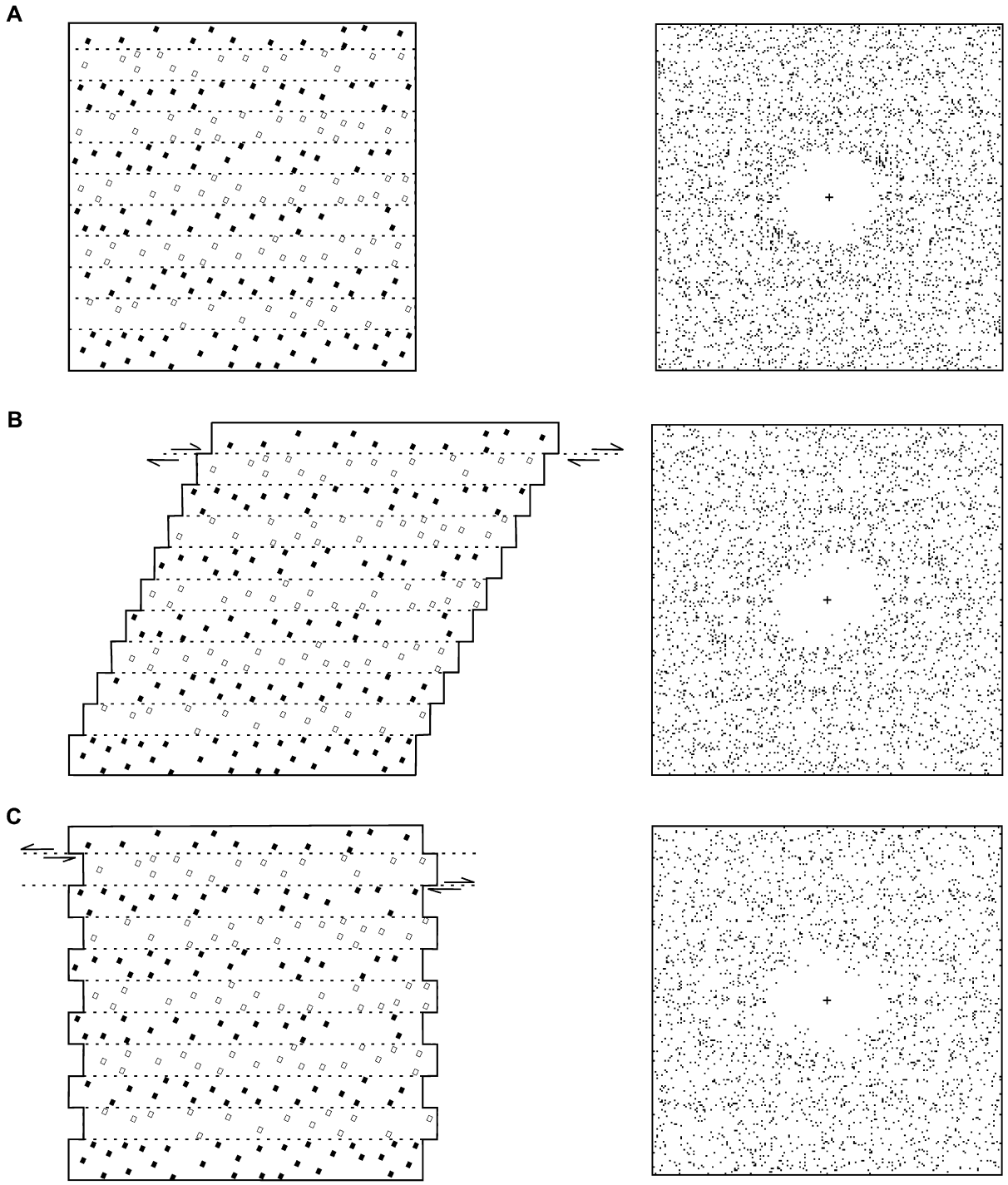

Fig. 11. Test of heterogeneous shearing along discrete shear planes (dashed lines). (A) Initial undeformed situation. (B) Displacement of feldspar trains by half of the mean distance between individual grains. The shear sense is constant from base to top. The corresponding Fry diagram gives an ellipse with a small eccentricity. (C) Displacement of feldspar trains by half of the mean distance between individual grains with periodic reversal of the shear sense. The corresponding Fry diagram is an ellipse with a small eccentricity.

4. The Fry method applied to a porphyritic orthogneiss

4.1. Geologic setting

The spatial distribution of crystals and the Fry method have been tested on the Randa porphyritic orthogneiss. It is included in the Siviez-Mischabel fold-nappe, in the Middle Penninic domain of the Western Swiss Alps. It derives from a subalcaline porphyritic Permian (late Variscan) granite dated at 269 ± 2 Ma (Bussy et al., 1996). It was deformed and metamorphosed during the Alpine Tertiary event under greenschist facies (~450 °C, 40–35 Ma; Steck and Hunziker, 1994). This orthogneiss displays a strong alpine foliation and at least two extension lineations (Steck, 1984, 1990; Markley et al., 1999).

It is mainly porphyritic with quartz and more frequently K-feldspars phenocrysts (see Thélin, 1987, for a more detailed petrographic description). The size of the K-feldspars phenocrysts varies from about 0.5 to 7 cm. They form an unpacked and unsorted aggregate. The K-feldspars phenocrysts are mostly monocrystalline but can also form polycrystalline aggregates of rectangular or ovoid shape. They mostly suffer a rigid deformation with crystallization of quartz-albite in the pressure shadows or in millimetric fractures (Thélin, 1987).

The Fry method is applied using K-feldspar phenocrysts at outcrop scale. Digital pictures of planar outcrops, approximately parallel to the lineation and perpendicular to the foliation, are the base of the present study. On this type of document, the large and pale K-feldspars phenocrysts contrast with the darker matrix (Fig. 12A).

4.2. Selection of phenocrysts

Image analysis software is now currently used (e.g. Ailleres and Champenois, 1994; Ailleres et al., 1995; Mukul, 1998; Heilbronner, 2000; Jerram et al., 2003; Perring et al., 2004) to determine various parameters of objects (shape, size or positional data) from a digital picture. In our study, the feldspar crystals were selected using the image analysis program ''AnalySIS Pro'' (Soft-Imaging System GmbH, Münster, Germany). The light-colored K-feldspars were selected using a threshold function, then the center of objects was automatically detected by the software. More than 2000 crystals can be selected in an outcrop digital picture. They are phenocrysts or are part of the matrix. For the Fry method, phenocrysts only have to be selected; therefore a size distribution analysis has been performed to discriminate between the population belonging to the matrix and one formed by phenocrysts. According to studies on crystal size distribution (Mock and Jerram, 2005; Gualda, 2006), at least 200–250 crystals are necessary to estimate the size distribution in a sample. Below this number, such a size selection is meaningless.

A normal probability plot was constructed with area values (directly given by the image analysis program) of the selected feldspars. On this graph, the area values are transformed into their corresponding normal score values (Nscore) and plotted versus the log of the area values (e.g. Kanevski and Maignan, 2004). The Nscore for an item indicates how far and in what direction, that item deviates from its distribution's mean, expressed in units of its distribution's standard deviation. If the obtained normal probability plot is approximately a straight line, it is reasonable to conclude that the values come from a population that is approximately normal.

The normal probability plots obtained with the area values of the selected feldspar crystals from the Randa orthogneiss pictures, display clearly two main populations (Fig. 12B). The dark straight line on the right of the plot underlines the population with the bigger crystals. This analysis provides a good assessment of the phenocryst population and can be used to select the crystals needed to perform the Fry method. Although there may be some error in the identification of small 2D sections through phenocrysts from ground mass crystals, or, according to the cases, some approximation due to the possibility for large shape variations in the phenocryst population (e.g. Mock and Jerram, 2005), the method has successfully identified 904 feldspars which correspond well with the observed phenocryst distribution (Fig. 12C), and provides a basis for the definition of crystal centers.

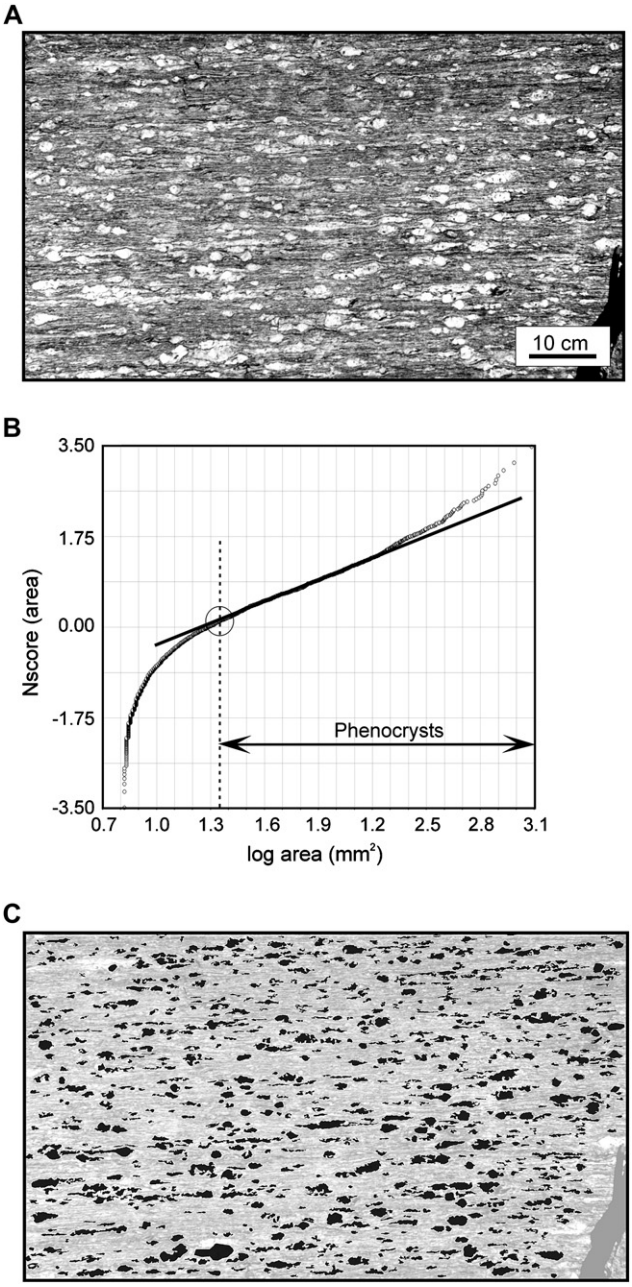

Fig. 12. Image analysis of an orthogneiss outcrop picture before using the Fry method. (A) Outcrop picture of the Randa porphyritic orthogneiss. Selection of all the feldspars was by image analysis (gray level threshold). More than 2000 objects were selected. (B) Normal probability plot of the size distribution (area) to discriminate between matrix and phenocrysts of the selected feldspar of (A). This plot clearly reveals two main populations. The dark straight line on the right of the plot defines the population of phenocrysts. (C) Corresponding selection of the feldspar phenocrysts in dark (904).

4.3. Spatial distribution of K-feldspar phenocrysts in the Randa orthogneiss

The different tests proposed in previous sections are now applied to the Randa orthogneiss. The Morishita diagram obtained for the 904 selected feldspar phenocrysts displays a homogenous distribution pattern (Fig. 13A). In conclusion, no clustering and no random distribution of the centers have been detected. In addition, the cumulative histogram of angles displays uniform and smoothed gradation, so an isotropic distribution of objects is therefore confirmed (Fig. 13B). Due to the large number of selected K-feldspar phenocrysts (904), the calculated angle values are numerous (816312), and only the cumulative histogram of the angles between 0° and 30° has been plotted.

According to these tests, the spatial distribution of K-feldspars phenocrysts in the Randa orthogneiss fits the necessary initial conditions for the application of the Fry method. Ideally, these tests should have been performed also on the undeformed granite and not only on the orthogneiss. To try to overcome the lack of an undeformed sector in the Randa orthogneiss, the Mte Capanne granite (Elba Island, Italy) was taken as a typical example for a tectonically undeformed porphyritic granite.

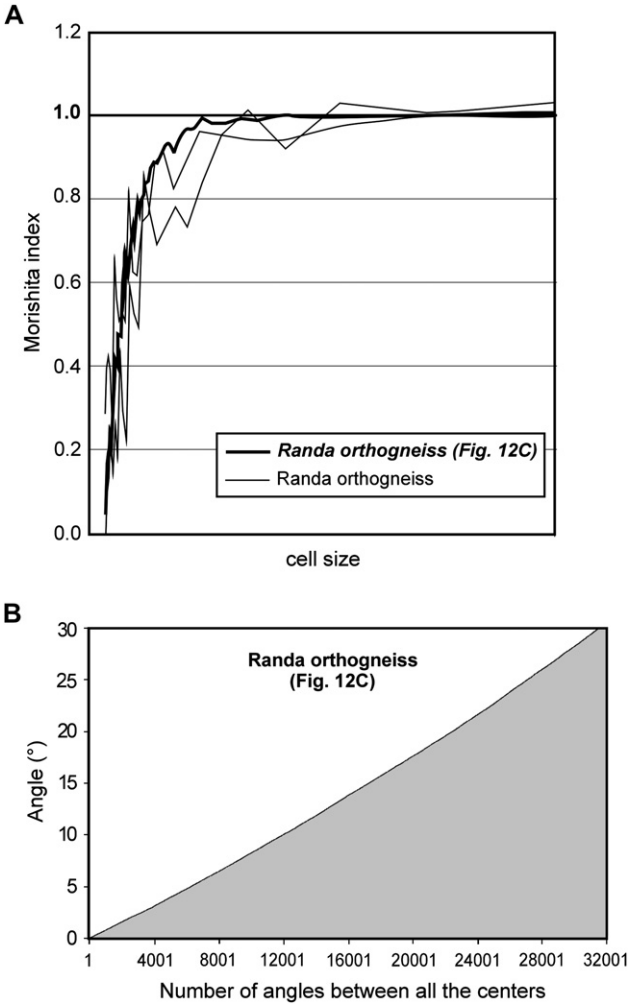

Fig. 13. (A) Morishita diagram for the Randa orthogneiss. Morishita index decreases together with cell size typical of a homogeneous distribution of K-feldspar phenocrysts. (B) Cumulative histogram of the angles between every 904 center position of the phenocrysts of Fig. 12C, typical of an isotropic distribution.

4.4. Spatial distribution of K-feldspar phenocrysts in the Mte Capanne granite

The Monte Capanne granite (Elba Island, Italy) is a subcircular pluton with a diameter of about 9 km, dated around 6 Ma (Saupé et al., 1982; Juteau et al., 1984). Most of this magmatic body, except its extreme rim, has escaped tectonic deformation after its emplacement (Bouillin, 1983; Bussy, 1990; Daniel and Jolivet, 1995). It contains numerous K-feldspars phenocrysts in a matrix composed mostly of biotite, quartz, K-feldspar and plagioclase (Marinelli, 1959; Bussy, 1990). K-feldspar phenocrysts are idiomorphic, 5 to 20 cm long (Fig. 14A), and much bigger than K-feldspars from the matrix (0.5–0.8 cm). These phenocrysts are clearly not deformed but are in many places preferentially oriented due to magmatic flow processes (Bouillin, 1983). This granite also contains a lot of subcircular and micro-grained enclaves (Bussy, 1991; Macera and Bruno, 1994). Digital pictures from undeformed zones of this granite, coming from the Capo San Andrea area, have been used for spatial and Fry analyses.

A Morishita diagram for the centers of the K-feldspar phenocrysts of the Mte Capanne granite demonstrates a homogenous distribution pattern (Fig. 14B). In addition, the cumulative histogram of the angular values displays a uniform and smoothed gradation that confirms an isotropic distribution (Fig. 14C). According to these tests, the K-feldspar phenocryst distribution is compatible with the Fry method. The same result is obtained also on outcrops with a moderate to clear preferred orientation of feldspars due to magmatic fluidal structure. Although more tests should be done on several porphyritic granites, we propose the conclusion that this type of rock can be used in a Fry analysis unless the contrary can be proved.

4.5. Fry diagrams for the Randa orthogneiss and the Mte Capanne granite

Center positions (coordinates) of the selected K-feldspar phenocrysts obtained from image analysis have been imported into the INSTRAIN 3.01 software developed by Erslev in 1993 (from Erslev, 1988; Erslev and Ge, 1990) to draw Fry diagrams. For the Randa orthogneiss, the vacancy field in the Fry diagram gives an ellipse with axial ratio of 2.8 in the example of Fig. 15A. Other strain ellipses have been estimated on outcrop sections parallel either to the L1 or L2 extension lineations. The axial ratios of the strain ellipses vary between 2.0 and 5.3. The measured finite strain using the Fry method could intuitively seems small compared with what can be expected in gneiss in an overturned limb of an alpine fold-nappe. But according to the tests proposed in the present paper, the

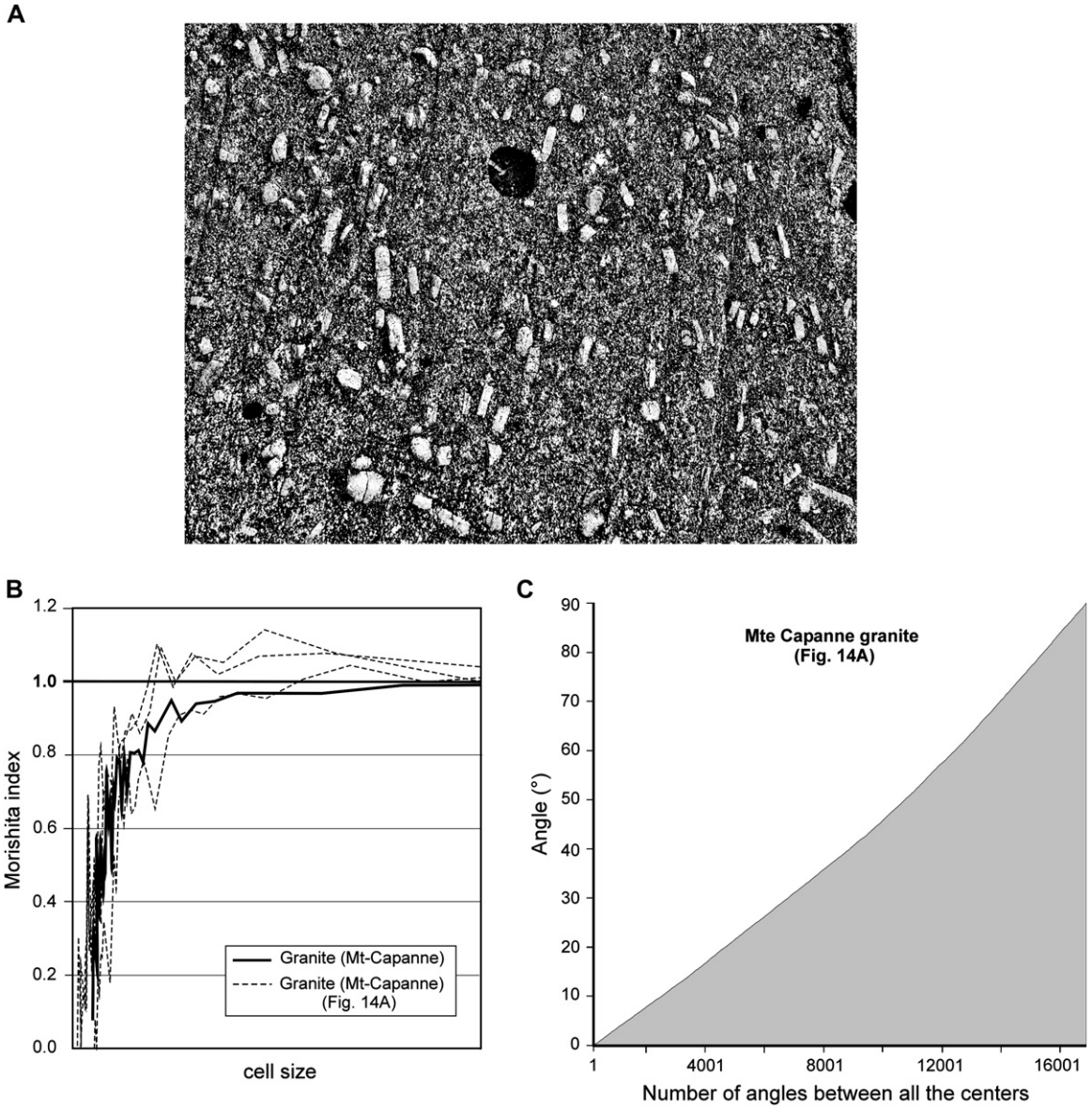

Fig. 14. (A) Outcrop picture of the Mte Capanne granite. The observed enclaves display a circular shape. (B) Morishita diagram for the Mte Capanne granite. Morishita index decreases together with cell size typical of a homogeneous distribution of K-feldspar phenocrysts. (C) Cumulative histogram of the angles between the phenocrysts of (A), typical of an isotropic distribution.

results of the Fry method in the Randa orthogneiss cannot be rejected on the base of a non-suitable distribution of points.

The influence of a possible heterogeneous deformation at outcrop scale has to be discussed. As demonstrated in a previous section, if deformation is mainly distributed on discrete shear-bands, the Fry method could greatly underestimate the overall finite strain (Fig. 11). If the foliation represents discrete shear zones (C-plane), the method is not applicable; however if it corresponds to a true schistosity (XY plane of the strain ellipsoid), the method can be used. In the case of the Randa orthogneiss, the main foliation consists in a rather penetrative schistosity, marked by elongated quartz zones and preferential orientation of phyllosilicates. It is possible also that part of the planar structure results from partial dissolution of quartz. Therefore, we consider that heterogeneous deformation by localized shear bands cannot be invoked to reject the Fry method results. Moreover, the Fry method will integrate other types of deformation heterogeneities. The strain values obtained at outcrop scale can be considered as representative.

The Fry method applied to the Mte Capanne granite displays diagrams with an almost circular vacancy field (Fig. 15B). This undeformed state is confirmed by the presence of subcircular micro-grained enclaves. A similar result is obtained even where a clear magmatic preferred orientation of crystals due to magmatic flow (Bouillin, 1983) is observed on several outcrops. Magmatic flow is the displacement of melt with rigid rotation of crystals in suspension (Paterson et al., 1989), and probably this phenomenon can be compared to heterogeneous simple shear deformation as described on Fig. 10 together with a rotation of crystals parallel to the

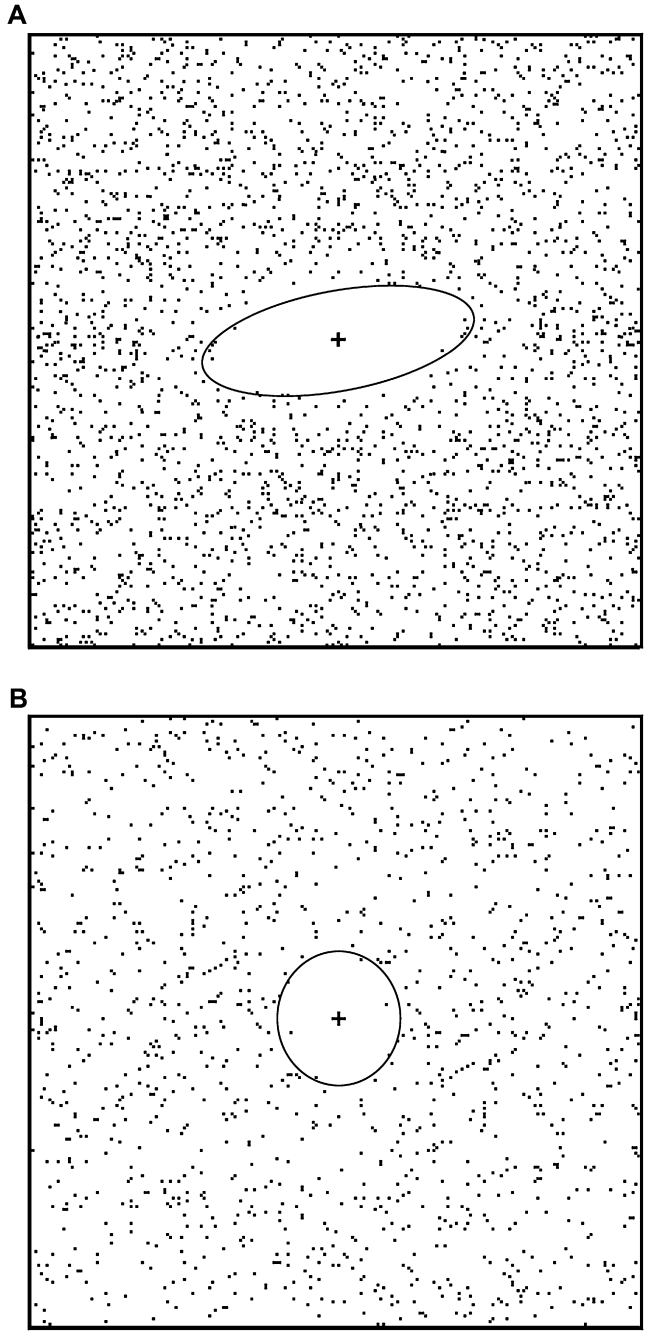

Fig. 15. (A) Strain ellipse obtained with the Fry method for the Randa orthogneiss (904 selected crystals of the Fig. 12C). (B) Strain ellipse obtained with the Fry method for the Mte Capanne granite. The result is a circle or an ellipse with small eccentricity.

flow direction. As discussed previously, the Fry method is mostly insensitive to this type of deformation. Therefore the Fry method will not record magmatic flow deformation but post-magmatic deformation only.

5. Conclusions

The Fry method was originally designed to measure strain in a packed aggregate of particles with similar shape and dimension. The distribution of K-feldspars in a porphyritic granite diverges from this simple initial situation. Even so the Fry method can be used to estimate strain in a deformed porphyritic granite (“augen orthogneiss”) providing several conditions and tests listed below. As a great number of points is required for a good quality Fry diagram, image analysis on digital pictures seems nowadays the necessary base document for such study.

1. K-feldspars phenocrysts can be selected by statistical size distribution study, using for example a normal probability plot.
2. The spatial distribution of points has to be tested for homogeneity and isotropy. The Morishita diagram is an efficient technique to check for homogeneity, while statistics on angles between points (cumulative histograms) can reveal anisotropy. Spatial distribution of K-feldspar phenocrysts in an undeformed porphyritic granite (Mte Capanne granite, Elba) and a deformed one (Randa “augen orthogneiss”) was found to be isotropic and homogeneous in both case.
3. The Fry method is insensitive to deformation distributed on discrete shear-bands. Strain associated with this type of deformation will not be detected by the method. This could be considered as a great disadvantage but on the other hand it presents the advantage that magmatic deformation associated with magmatic fluidal foliation will be ignored. Therefore, strain measured in an orthogneiss will not be influenced by inherited magmatic structures.

The Fry method was successfully applied to the Randa orthogneiss and has given strain ellipses with axial ratio from 2.8 to about 5.3. Detailed interpretation of the strain distribution in this orthogneiss and this area will be given in a future paper.

Acknowledgments

Fruitful discussions and critical reading of the manuscript by Rick Groshong and Arthur Escher were highly appreciated. We thank Eric A. Erslev for providing us with the INSTRAIN software. Mikhail Kanevski and Aziz Chaouch helped with the statistical analysis. We thank also Henri Masson, Albrecht Steck and François Bussy, for numerous discussions and constant encouragement, and Philippe Thélin for the introduction to the Randa granite. The authors would like to thank Susan H. Treagus and Dougal Jerram for constructive reviews of the manuscript. The Swiss National Science Foundation (grants 2100-066983 and 200020-105506) is gratefully acknowledged for financial support.

References

Ailleres, L., Champenois, M., 1994. Refinements to the Fry method (1979) using image processing. Journal of Structural Geology 16 (9), 1327–1330.
Ailleres, L., Champenois, M., Macaudiere, J., Bertrand, J.M., 1995. Use of image analysis in the measurement of finite strain by the normalized Fry

method; geological implications for the "Zone Houillère" (Briançonnais zone, French Alps). Mineralogical Magazine 59 (2), 179–187.

Bouillin, J.-P., 1983. Exemples de déformations locales liées à la mise en place de granitoïdes alpins dans des conditions distensives: L'île d'Elbe (Italie) et le Cap Bougaroun (Algérie). Revue de Géologie Dynamique et de Géographie Physique 24 (2), 101–116.

Bussy, F., 1990. Pétrogenèse des enclaves microgrenues associées aux granitoïdes calco-alcalins: exemple des massifs varisque du Mont-Blanc (Alpes occidentales) et miocène du Monte Capanne (Ile d'Elbe, Italie). Mémoires de Géologie (Lausanne) 7.

Bussy, F., 1991. Enclaves of the Late Miocene Monte Capanne Granite, Elba Island, Italy. In: Didier, J., Barbarin, B. (Eds.), Enclaves and Granite Petrology. Developments in Petrology, 13. Elsevier, Amsterdam, pp. 167–178.

Bussy, F., Sartori, M., Thélin, P., 1996. U-Pb zircon dating in the middle Penninic basement of the Western Alps (Valais, Switzerland). Schweizerische Mineralogische und Petrographische Mitteilung 76 (1), 81–84.

Crespi, J.M., 1986. Some guidelines for the practical application of Fry's method of strain analysis. Journal of Structural Geology 8 (7), 799–808.

Daniel, J.-M., Jolivet, L., 1995. Detachment faults and pluton emplacement: Elba Island (Tyrrhenian Sea). Bulletin de la Société géologique de France 166 (4), 341–354.

Dunne, W., Onasch, C.M., Williams, R.T., 1990. The problem of strain-marker centers and the Fry method. Journal of Structural Geology 12 (7), 933–938.

Erslev, E.A., 1988. Normalized center-to-center strain analysis of packed aggregates. Journal of Structural Geology 10 (2), 201–209.

Erslev, E.A., Ge, H., 1990. Least-squares center-to-center and mean object ellipse fabric analysis. Journal of Structural Geology 12 (8), 1047–1059.

Fry, N., 1979. Random point distributions and strain measurement in rocks. Tectonophysics 60 (1–2), 89–105.

Gualda, G.A.R., 2006. Crystal Size Distributions Derived from 3D Datasets: Sample Size Versus Uncertainties. Journal of Petrology 47, 1245–1254.

Heilbronner, R., 2000. Automatic grain boundary detection and grain size analysis using polarization micrographs or orientation images. Journal of Structural Geology 22 (7), 969–981.

Jerram, D.A., Cheadle, M.J., 2000. On the cluster analysis of grains and crystals in rocks. American Mineralogist 85, 47–67.

Jerram, D.A., Cheadle, M.J., Hunter, R.H., Elliott, M.T., 1996. The spatial distribution of grains and crystals in rocks. Contributions to Mineralogy and Petrology 125, 60–74.

Jerram, D.A., Cheadle, M.J., Philpotts, A.R., 2003. Quantifying the building blocks of igneous rocks: are clustered crystal frameworks the foundation? Journal of Petrology 44, 2033–2051.

Juteau, M., Michard, A., Zimmermann, J.L., Albarède, F., 1984. Isotopic heterogeneities in the granitic intrusion of Monte Capanne (Elba Island, Italy) and dating concepts. Journal of Petrology 25, 532–545.

Kanevski, M., Maignan, M., 2004. Analysis and Modelling of Spatial Environmental Data. EPFL Press, Lausanne.

Kanevski, M.F., Demyanov, V., Chernov, S., Savelieva, E., Timonin, V., Maignan, M., 1998. Environmental spatial data analysis with Geostat Office software, in: Buccianti, A., Nardi, G., Potenza, R. (Eds.), Proceedings of IAMG '98 (the fourth annual conference of the International Association for Mathematical Geology), Napoli, 4, pp. 161–166.

Korvin, G., 1992. Fractal Models in the Earth Sciences. Elsevier, Amsterdam.

Kretz, R., 1969. On the spatial distribution of crystals in rocks. Lithos 2 (1), 39–66.

Lacassin, R., Van den Driessche, J., 1983. Finite strain determination of gneiss; application of Fry's method to porphyroid in the southern Massif Central (France). Journal of Structural Geology 5 (3–4), 245–253.

Macera, P., Bruno, A., 1994. Geochemical and isotopic (Sr-Nd) investigation on the Mt. Capanne Pluton (Elba Island) and its mafic enclaves, in: Bortolotti, V., Chiari, M. (Eds.), Proceedings of the 76th summer meeting of the Societa Geologica Italiana; The Northern Apennines; Part 2, The Neogene basins, the Neogene-Quaternary evolution, the minerogenetic processes. Memorie della Societa Geologica Italiana 48, pp. 695–697.

Marinelli, G., 1959. Le intrusioni terziarie dell'Isola d'Elba. Atti della Società Toscana di Scienze Naturali 66A, 50–253.

Markley, M.J., Teyssier, C., Caby, R., 1999. Re-examining Argand's view of the Siviez-Mischabel nappe. Journal of Structural Geology 21 (8–9), 1119–1124.

McNaught, M.A., 1994. Modifying the normalized Fry method for aggregates of non-elliptical grains. Journal of Structural Geology 16 (4), 493–503.

McNaught, M.A., 2002. Estimating uncertainty in normalized Fry plots using a bootstrap approach. Journal of Structural Geology 24 (2), 311–322.

Mock, A., Jerram, D.A., 2005. crystal size distributions (CSD) in three dimensions: insights from the 3D reconstruction of a highly porphyritic rhyolite. Journal of Petrology 46, 1525–1541.

Mock, A., Jerram, D.A., Breitkreutz, C., 2003. Using quantitative textural analysis to understand the emplacement of shallow-level rhyolitic laccoliths - a case study from the Halle Volcanic Complex, Germany. Journal of Petrology 44, 833–849.

Morishita, M., 1959. Measuring of the dispersion of individuals and analysis of the distributional patterns. Memoir of the Faculty of Sciences. In: serie E, 2. Kyushu University, pp. 215–235.

Mukul, M., 1998. A spatial statistics approach to the quantification of finite strain variation in penetratively deformed thrust sheets; an example from the Sheeprock thrust sheet, Sevier fold-and-thrust belt, Utah. Journal of Structural Geology 20 (4), 371–384.

Onasch, C.M., 1986. Ability of the Fry method to characterize pressure-solution deformation. Tectonophysics 122 (1–2), 187–193.

Paterson, S.R., Vernon, R.H., Tobisch, O.T., 1989. A review of criteria for the identification of magmatic and tectonic foliations in granitoids. Journal of Structural Geology 11 (3), 349–363.

Perring, C.S., Barnes, S.J., Verall, M., Hill, R.E.T., 2004. Using automated digital image analysis to provide quantitative petrographic data on olivine-phyric basalts. Computers and Geosciences 30, 183–195.

Ramsay, J.G., Huber, M.I., 1983. Techniques of Modern Structural Geology. Academic Press, London.

Rey, D., 2002. Shear2F: un logiciel de modélisation tectonique. Mémoires de Géologie (Lausanne) 37.

Saupé, F., Marignac, Ch, Moine, B., Sonet, J., Zimmermann, J.L., 1982. Datation par les méthodes K/Ar et Rb/Sr de quelques roches de la partie orientale de l'Ile d'Elbe (province de Livourne, Italie). Bulletin de Minéralogie 105, 236–245.

Steck, A., 1984. Structures de déformations tertiaires dans les Alpes centrales (transversale Aar-Simplon-Ossola). Eclogae Geologicae Helvetiae 77 (1), 55–100.

Steck, A., 1990. Une carte des zones de cisaillement ductile des Alpes centrales. Eclogae Geologicae Helvetiae 83 (3), 603–627.

Steck, A., Hunziker, J., 1994. The Tertiary structural and thermal evolution of the Central Alps; compressional and extensional structures in an orogenic belt. Tectonophysics 238 (1–4), 229–254.

Thélin, P., 1987. Nature originelle des gneiss oeillés de Randa (Nappe de Siviez-Mischabel, Valais). Mémoires de la Société vaudoise des Sciences naturelles 18.

Treagus, S.H., Treagus, J.E., 2002. Studies of strain and rheology of conglomerates. Journal of Structural Geology 24 (10), 1541–1567.